RSC Advances

ROYAL SOCIETY OF CHEMISTRY

www.rsc.org/advances

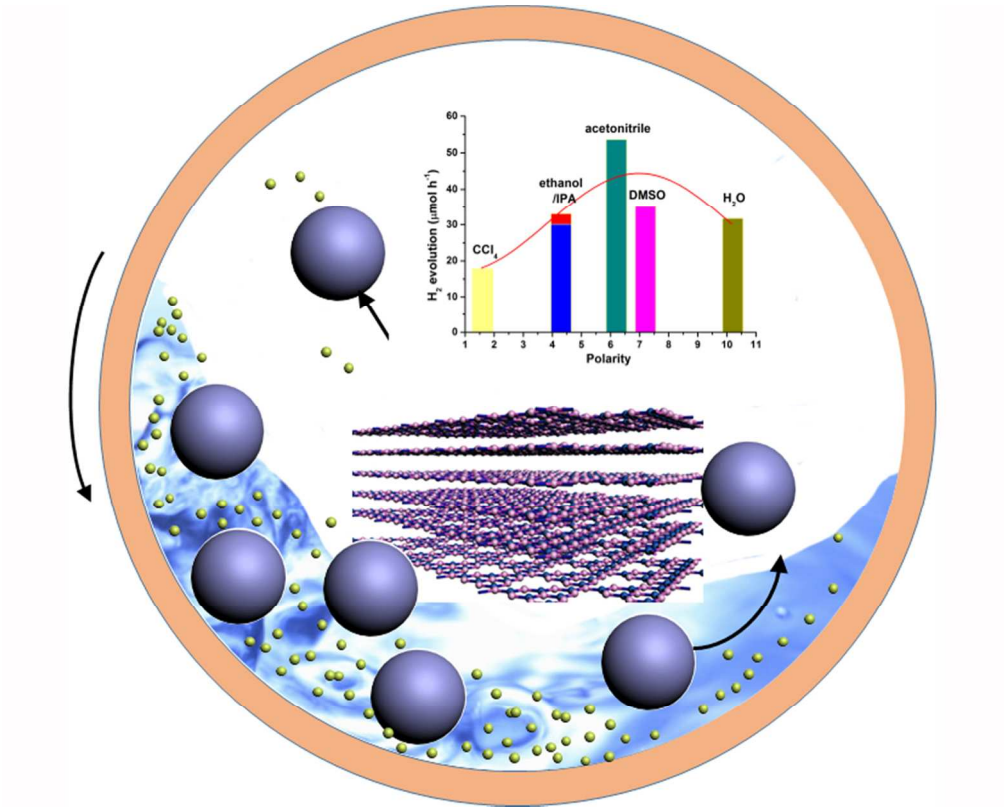

Graphitic-C3N4 with disordered structure was processed for the first time by a liquid-assisted planetary ball milling approach.

Cite this: DOI: 10.1039/c0xx00000x

www.rsc.org/xxxxxx

ARTICLE TYPE

Structure disorder of graphitic carbon nitride induced by liquid-assisted grinding for enhanced photocatalytic conversion

Xue Lu Wang, [a,b] Wen Qi Fang,[a,c] Shuang Yang,[a] Pengfei Liu,[a] Huijun Zhao* [b] and Hua Gui Yang* [a,b]

Received (in XXX, XXX) Xth XXXXXXXXX 20XX, Accepted Xth XXXXXXXXX 20XyX

DOI: 10.1039/b000000x

Graphitic-C_3N_4 with disordered structure was processed for the first time by a liquid-assisted planetary ball milling approach. Through this simple and effective mechanochemistry method, the milled samples displayed outstanding visible-light photoactivity and the optimized one showed 7-fold higher H_2 evolution rate than the bulk one.

Mechanochemistry, which can be trace back to the antiquity (4th century BC), has seen a huge upsurge of interest in recent years and now is emerging as an excellent environmentally friendly alternative to traditional solution-based approaches in a number of industries.[1] Generally, mechanochemistry is defined as a "Chemical reaction that is induced by the direct absorption of mechanical energy" with methods of shearing, stretching, and grinding – typically carried out using a mortar and pestle, or a ball mill within which the powder reagents are shaken violently together with stainless-steel balls in a sealed vessel.[2] Subsequently, the developments have been aided by new mechanochemical techniques where the reactivity of the precursors mixture is improved by the addition of sub-stoichiometric amounts of liquids.[3] The use of liquid-assisted grinding (LAG) reveals an unexpected ability to selectively and quantitatively construct diverse materials from the same precursors.

For microscopic understanding the mechanism of the traditional mechanochemical reactions, it is relevant to note the physical effects and the chemical reaction which grinding can have. Several pieces of experimental evidence have been summarized below, (a) particles diminish and expose fresh surfaces, (b) intimate mixing of reactants, introducing disordered defects, amorphization, and polymorphic transformations, and (c) frictional heating, both local and bulk.[2] However, in the case of a reaction involving only one reactant, the improved intimacy of contact between different reactants is not a factor. The enhanced kinetically reactions by the presence of a liquid points to a more active role for the liquid, in which the liquid increases the rate of diffusion of molecules from the reactant to the product phase, and this rate enhancement increases rapidly with the decrease in reactant particle size that occurs with grinding. But for dry mechanochemical reactions, an increase in temperature can be caused by frictional heating of the solid during high energy mechanical milling in a ball mill which will bring more side effect because of the high temperature.[2,4]

Mechanochemical method can create defects, specific to oxides, such as Schottky or Frenkel defects or crystallographic shear planes (Wadsley defects).[5] At the same time, organic molecular crystals are very different in some respects from metals or inorganic oxides. The crystal structure of organic solid are generally anisotropic, thus, the shapes of particles are far from being isometric and different properties can be attributed to the different crystal faces. A unique feature of the organic molecular crystals mainly reflects in the co-existence between the strong covalent intramolecular bonds and several types of weaker intermolecular interactions. Mechanical treatment could selectively activate some types of bonds which remains challenges by traditional methods.[6] Nevertheless, as for the field of photocatalysis, the structure disorder and surface defects could provide trapping site for photoinduced carriers and hinder the recombination of electrons and holes, hence improving overall quantum efficiency.[7] Thus, mechanochemical method can be regarded as an available pathway to treat and synthesize photocatalyst with low cost and large scale.

Herein, we first introduced this improved mechanochemical approach, designated LAG, in construction of graphitic carbon nitride (g-C_3N_4) with numerous bulk and surface defects. The g-C_3N_4 with a graphite-like structure is an efficient, simple, and sustainable photocatalytic material working with visible light, and the catalytic activity of which is closely related to its defects and termination sites of the sheet.[8] Thus, defects and structure disorder may be significant influence factors on its photocatalytic performance, as well as electronic structure, charge transport and surface properties. It is well known that LAG with different solvents may have different effects, which is significantly influenced by the surface tensions of them.[2] The adhesion between the g-C_3N_4 and the liquid along with the impact force lead to some advantageous structure and surface defects with the

Table 1 Physicochemical properties of CN and LAG-CN-x samples.

Catalyst	Solvent	Polarity	C/N atmomic	S_{BET}[a] [$m^2\ g^{-1}$]	HER[b] [$\mu mol\ h^{-1}$]
CN	/	/	0.675	5.1	8.53
LAG-CN-1	H_2O	10.2	0.680	23.7	31.76
LAG-CN-2	CCl_4	1.6	0.686	15.9	17.84
LAG-CN-3	ethanol	4.3	0.678	23.9	33.05
LAG-CN-4	IPA	4.3	0.678	22.7	30.14
LAG-CN-5	acetonitrile	6.2	0.678	21.6	53.61
LAG-CN-6	DMSO	7.2	0.680	9.6	35.14

[a] The surface area; [b] H_2 evolution rate (30 mg).

cooperation of the shearing, stretching and grinding.

The LAG samples were synthesized by ball milling g-C_3N_4 in the presence of different organic solvents (see details in Supplementary Information Section 1). Through this simple and effective mechanochemistry approach, bulk g-C_3N_4 might be transformed into some smaller, compressed, or squeezing pieces with some vacancy or other disordered activation defects, and all obtained samples show good dispersion in the water. For simplicity, the resulting LAG samples were denoted as LAG-CN-x, where x is an arbitrary number that represents the organic solvents with different polarities (see Table 1). The polarities we chose here are spanning from 1.6 to 10.2. Among all the solvent, acetonitrile seem to be a more promising candidate with appropriate surface tension (~29 N m^{-1}).[9] Considering the complexity of the solvent itself, we will focus on analysing and comparing the typical samples of CN, LAG-CN-1, and LAG-CN-5.

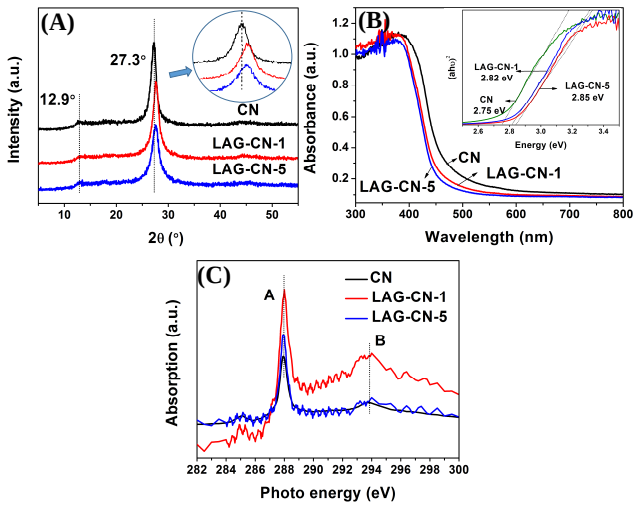

Fig. 1 XRD patterns (A), UV-vis absorption spectra (B), the bandgap determination (B, inset), and the C K-edge XANES spectra (C) of CN, LAG-CN-1 and LAG-CN-5 samples.

The texture and chemical structure of the samples were characterized with various physical and chemical techniques. Carbon and nitrogen stoichiometry of the samples was determined by elemental analysis (Table 1). It should be noted that, according to the EL results, the atomic C/N molar ratios of LAG-CN-x samples are higher than CN, but lower than that of the theoretical value of the ideal crystal g-C_3N_4. Taking LAG-CN-5 for example, the bulk atomic C/N ratio has increased from pristine 0.675 to 0.678 for the LAG-CN-5. However, the surface atomic ratio of C to N increases from 0.80 to 0.90 according to the percentages of C and N determined by XPS. Obviously, the surface of LAG-CN-5 is poorer in nitrogen than CN, indicating that mechanical milling may result in the surface defects (nitrogen loss) with the assistance of the organic solvent and led to the increase in the BET surface area.[10] However, there are not a positive correlation between the increased BET surface area and the hydrogen production. Accordingly, the activation defects play a significant role in the whole process.

Fig. 1A shows the XRD patterns of CN, LAG-CN-1 and LAG-CN-5 samples. A highly resembled structure can be determined, with the arising of reflection peaks (002) and (100) at ~27.3° and ~12.9°, respectively. The dominate characteristic interlayer stacking peak of the π-conjugated aromatic system of LAG-CN-x, indexed for graphitic like materials as the (002) peak, slightly up-shift; that is, the average interlayer distance of the LAG-CN-x is notably compressed to a smaller d-spacing value, according to Bragg`s law. The reaction upon LAG presumably could influence the conformation and the connectivity of the resultant sheets, ascribed to the shear stress and the impact-induced local heating and high local pressures. This can proved that there existed some structure disorder and surface defects after LAG. The tendency offers an important tool to tune the physical and chemical properties of the samples, and hence to adjust their photocatalytic performance.[8,11]

As estimated from the UV-vis spectrum (Fig. 1B and Fig. S1), the optical absorption edges of LAG-CN-x presents blue shifts compared with that of CN, corresponding to an increase in band gap from 2.75eV of CN to 2.85eV of LAG-CN-5. Generally, the blue shifts can be attributed to the decreased conjugation length or quantum confinement effects of the samples. Moreover, the hypsochromic-shift performance of LAG-CN-x is presumably due to the strong quantum confinement effects, because of the enhanced surface area.[11] Moreover, the hypsochromic-shift performance of LAG-CN-x in the spectrum can be due to an H-aggregates type intermolecular packing between the layers.[12]

Looking at the C K-edge XANES spectra in Fig. 1C, the samples all exhibit two distinct peak at round 288 (A) and 294 eV (B). The signal A is attributed to the sp2-bonded carbon in N-containing aromatic rings (N-C=N) which is regarded as the major carbon species in the g-C_3N_4 polymer. The intensity of it for the LAG-CN-x sample is found to be higher than that of bulk CN, indicating the compressed average interlayer distance and the disordered structure. On the other hand, the feature B is related to interlayer states or transitions to sp3 hybridized states due to hydrogenation or oxygenated groups.[13] Additionally, the TEM images of CN, LAG-CN-1 and LAG-CN-5 are shown in Fig. 2. They all display the typical layered silk structure and similar to the results of the nitrogen adsorption-desorption experiments.

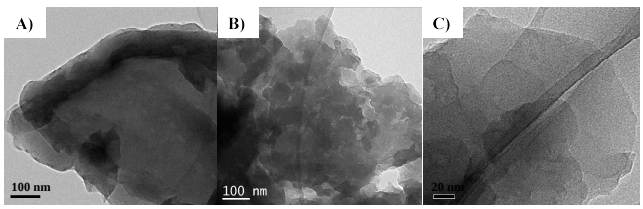

Fig. 2 TEM images of CN, LAG-CN-1 and LAG-CN-5 samples.

Typical FTIR spectra of the samples are displayed in Fig. 3. All of the characteristic vibration modes show that the spectra of the three samples are highly similar. The set of peaks between 1200 and 1700 cm^{-1} is assignable to the feature-distinctive stretch modes of tri-s-triazine heterocyclic ring (C_6N_7) unites, while the sharp peak at ~807 cm^{-1} is ascribed to their breathing mode. The broad bands in the range of the 3000-3700 cm^{-1} region can be

interpreted as the residual N-H components and the O-H bands, suggesting the partial hydrogenation of some nitrogen atoms and the surface-absorbed H_2O molecules, respectively. In comparison with CN, the vibrations of LAG-CN-1 and LAG-CN-5 become slightly stronger. Generally, the enhanced absorption peak around the region is presumably assigned to the absorbed H_2O and the weak uncondensed amine groups. However, there is no H_2O in the grinding environment of LAG-CN-5, thus, we attribute the enhancement to the distorted incomplete structure (disordered defects). Notably, the whole adsorption peak of LAG-CN-5 becomes a partly blue-shift compared with the CN. As we all know, the hypsochromic-shift is largely induced by the inductive effect, which may change the size, shape and density distribution of its electron cloud, and the spatial effects. Therefore, the shift would be regard as the generation of surface defects and the distorted structure caused by LAG. Moreover, the absence of –CN bonds near 2200 cm^{-1} excludes the possibility of self trimerzation of the –CN group in acetonitrile. This strongly indicates that acetonitrile only acts as a subcritical solvent to mediate the grinding, but involved in the chemical reaction.[14]

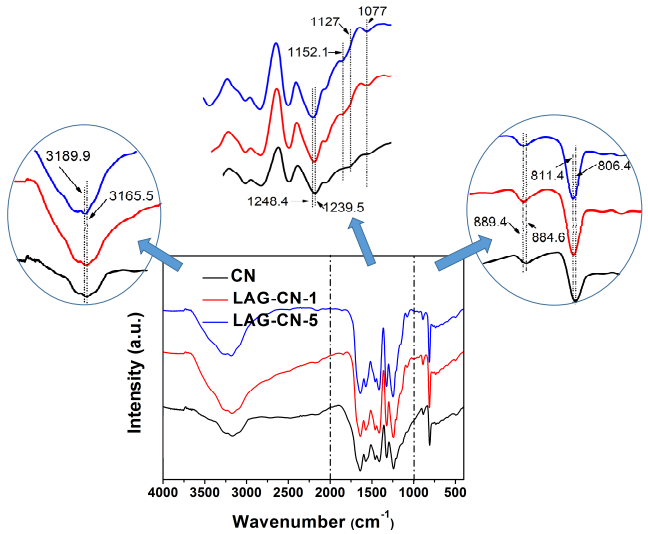

Fig. 3 FTIR spectra of CN, LAG-CN-1 and LAG-CN-5 samples.

In the XPS survey spectrum (Fig. S2A), all show three elements (C, N and O). This gives evidence that the LAG samples remain the same framework with the CN. A similar tendency is observed for the C1s signals (Fig. S2B), which were deconvoluted into three peaks at binding energies of 284.8 eV, 288.3 eV and 289. 4 eV, which can be ascribed to the sp2 C-C bonds, N=C-N coordination and the C-O groups induced by unavoidable oxidation of the samples, repectively. The N1s spectra in Fig. S2C show three peaks centering at 398.7, 399.8 and 401.1 eV. The dominance of the main peak (398.7 eV) originating from the sp2-hybridized nitrogen involved in triazine rings (C-N=C). The two peaks at about 399.8 and 401.1 eV can be ascribed to tertiary nitrogen (N-$(C)_3$) and amino functional groups having a hydrogen atom (C-N-H), respectively. The presence of the C-N-H groups originates from the incomplete condensation of the poly(tri-s-triazine) structures.[8, 15]

The larger bandgaps by 0.07 eV and 0.1 eV of the LAG-CN-1 and LAG-CN-5 compared to CN are further confirmed by the blue shift of the fluorescence emission by 8 nm and 13 nm, respectively (Fig. S3). This might be attributed to the quantum confinement effect by shifting the conduction and valence band edges in opposite directions.[10]

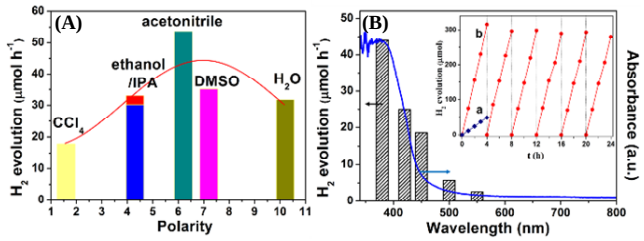

Fig. 4 (A) The rate of H_2 evolution on LAG-CN-x samples prepared with different polarity organic solvent LAG under visible-light irradiation (λ > 420 nm). (B) Steady rate of H_2 production in aqueous triethanolamine solution (10 vol%) by 50 mg 3.0 wt% Pt-deposited LAG-CN-5 samples as a function of wave-length of the incident light. Ultraviolet-visible absorption spectrum of the catalyst is also shown for comparison. Inset is the stability test of (b) 3.0 wt% Pt-deposited LAG-CN-5 for H_2 production under visible light, the (a) CN samples is also shown for comparison.

The photocatalytic performance of the as-prepared samples were evaluated by H_2 evolution under visible light irradiation (Fig. 4A). Notably, all samples show an enhanced H_2 evolution rate (HER) over CN to varying extents, and LAG-CN-5, with a 4.9% apparent quantum efficiency at 420 nm, shows the highest activity for its suitable polarity of acetonitrile solvent. Simultaneously, in order to confirm the inference, we also chose two solvents with the similar polarity (4.3). As expected, the two samples exhibit the close HER. Thus, polarity is of course one of the important influence factors that affect the mechanochemical process as well as the final products in LAG. However, more details investigations are still needed for real quantitative statements.

The durability of the LAG-CN-5 sample was evaluated in a water/triethanolamine solution (see the details in Section S1) by a 24 h experiment with intermittent evacuation every 4 h under visible light (>420 nm). As presented in Fig. 4B (inset), the H_2 produced increases steadily without noticeable deterioration of the activity. The turnover number with respect to the melem units and Pt atoms are 3.19 and 115.3, respectively, clearly indicating that the reaction indeed proceeds catalytically. Additionally, wavelength dependence of the photocatalytic H_2 evolution was performed on LAG-CN-5, and different monochrome filters were used. As depicted in Fig. 4B, the H_2 evolution rates match well with the diffuse reflectance spectra. The active wavelength is actually prolonged to wavelengths as long as 550 nm.

In summary, structure disordered g-C_3N_4 samples were successfully synthesized by a facile LAG approach. The cooperative effect of shearing, stretching and grinding reforms the structure and surface of g-C_3N_4. The resulting LAG-CN samples, therefore, harbour widen the bandgap, selectively activation of some defect points, and lead to a very good photoctalytic activity for hydrogen evolution under visible light.

Although mechanochemistry has historically been a sideline approach to synthesis, but its practicality, advantage and effectivity all can move it into the mainstream within the realm of chemical research.

Acknowledgements

We thank Prof. Caihao Hong for the valuable discussion on XANES. This work was financially supported by National Natural Science Foundation of China (21373083, 21203061), SRF for ROCS, SEM, SRFDP, Programme for Professor of Special Appointment (Eastern Scholar) at Shanghai Institutions of Higher Learning, Shanghai Municipal Natural Science Foundation (12ZR1407500), Fundamental Research Funds for the Central Universities (WD1313009 , WM1314018 , WD1214036), and China Postdoctoral Science Foundation (2012M511056, 2013T60425).

Notes and references

[a] *Key Laboratory for Ultrafine Material of Ministry of Education, School of Materials Science and Engineering, East China University of Science and Technology, Shanghai, 200237, China. Fax: +86-21-64252127; Tel: +86-21-64252127; E-mail: hgyang@ecust.edu.cn*

[b] *Centre for Clean Environment and Energy, Gold Coast Campus, Griffith University, Queensland, 4222, Australia. E-mail: h.zhao@griffith.edu.au*

[c] *QLD Micro- and Nanotechnology Centre, Griffith University, Nathan Campus, QLD 4111, Australia*

† Electronic Supplementary Information (ESI) available: Experimental details, UV-vis adsorption spectra, XPS spectra, fluorescence emission spectra and TEM images. See DOI: 10.1039/b000000x/

1 (a) L. Takacs, *J. Mineral Met. Mater. Soc.*, 2000, **52**, 12; (b) K. D. M. Harris, *Nat. Chem.*, 2013, **5,** 12-14.

2 (a) S. L. James, C. J. Adams, C. Bolm, D. Braga, P. Collier, T. Friscic, F. Grepioni, K. D. M. Harris, G. Hyett, W. Jones, A. Krebs, J. Mack, L. Maini, A. G. Orpen, I. P. Parkin, W. C. Shearouse, J. W. Steed and D. C. Waddell, *Chem. Soc. Rev.*, 2012, **41,** 413-447; (b) G. A. Bowmaker, *Chem. Commun.*, 2013, **49,** 334-348.

3 T. Friscic, I. Halasz, P. J. Beldon, A. M. Belenguer, F. Adams, S. A. J. Kimber, V. Honkimaki and R. E. Dinnebier, *Nat. Chem.*, 2013, **5,** 66-73.

4 L. Takacs, *Prog. Mater. Sci.*, 2002, **47,** 355-414.

5 (a) V. Sepelak, I. Bergmann, S. Kipp and K. D. Becker, *Z. Anorg. Allg. Chem.*, 2005, **631,** 993; (b) V. Sepelak, A. Düvel, M. Wilkening, K. Becker and P. Heitjans, *Chem. Soc. Rev.*, 2013, **42,** 7507-7520.

6 (a) E. Boldyreva, *Chem. Soc. Rev.*, 2013, **42,** 7719; (b) C. F. Burmeister, A. Kwada, *Chem. Soc. Rev.*, 2013, **42,** 7660.

7 X. B. Chen, L. Liu, P. Y. Yu and S. S. Mao, *Science*, 2011, **331,** 746.

8 (a) X. Wang, K. Maeda, A. Thomas, K. Takanabe, G. Xin, J. M. Carlsson, K. Domen and M. Antonietti, *Nat. Mater.*, 2009, **8,** 76-80; (b) A. Thomas, A. Fischer, F. Goettmann, M. Antonietti, J. Müller, R. Schlöql and J. M. Carlsson, *J. Mater. Chem.*, 2008, **18,** 4893-4908.

9 G. Korosl and E. Kovats, *J. Chem. Eng. Data*, 1981, **26,** 323-332.

10 P. Niu, L. Zhang, G. Liu, H. Cheng, *Adv. Funct. Mater.*, 2012, **22,** 4763-4770.

11 Y. Cui, J. Zhang, G. Zhang, J. Huang, P. Liu, M. Antonietti and X. Wang, *J. Mater. Chem.*, 2011, **21,** 13032-13039.

12 (a) X. H. Li, J. Zhang, X. Chen, A. Fischer, A. Thomas, M. Antonietti, *Chem. Mater.*, 2011, **23,** 4344-4348; (b) Y. Cui, J. Zhang, G. Zhang, J. Huang, M. Antonietti, *J. Mater. Chem.*, 2011, **21,** 13032-13039.

13 (a) L. Liu, T. K. Sham, W. Han, Phys. Chem. Chem. Phys., 2013, 15, 6929-6934; (b) N. Hellgren, J. Guo, Y. Luo, C. Såthe, A. Agui, S. Kashtanov, J. Nordgren, H. Ågren, J. E. Sundgren, *Thin Solid Film*, 2005, **471,** 19-34.

14 Y. Cui, Z. Ding, X. Fu and X. Wang, *Angew. Int. Ed. Chem.*, 2012, **51,** 11814-11818.

15 G. Zhang, J. Zhang, M. Zhang and X. Wang, *J. Mater. Chem.*, 2012, **22,** 8083-8091.

